ELSEVIER

Journal of Nuclear Materials 301 (2002) 90–97

journal of nuclear materials

www.elsevier.com/locate/jnucmat

Reaction of Zircaloy-4 with tellurium under different oxygen potentials

T. Arima *, T. Masuzumi, H. Furuya, K. Idemitsu, Y. Inagaki

Faculty of Engineering, Institute of Environmental Systems, Kyushu University, 6-10-1 Hakozaki, Fukuoka 812-8581, Japan

Received 1 May 2001; accepted 12 December 2001

Abstract

Corrosion behavior of Zircaloy-4 has been studied under different oxygen potentials and tellurium vapor pressures. The oxygen potential was controlled by buffer over the range of −600 to −430 kJ/mol. Under the condition of oxygen potential of less than −500 kJ/mol with coexisting tellurium vapor, duplex corrosion layers were formed on the surface of Zircaloy-4 specimens, which consisted of zirconium telluride and zirconium oxide. The thickness of corrosion layer was increased with tellurium vapor pressure. For the oxygen potential over −430 kJ/mol, only zirconium oxide was observed on the specimen surface regardless of coexistence of tellurium vapor. © 2002 Elsevier Science B.V. All rights reserved.

PACS: 28.41.T

1. Introduction

Tellurium is one of the fission products from fissile material, uranium and plutonium. And its fission yield is relatively high. The chemical properties are characterized by low melting temperature of 450 °C and high volatility. Furthermore, under the irradiation condition, tellurium is a precursor of radiotoxic iodine. In the normal operating fuel rods, the chemical form of tellurium is predicted to be Cs_2Te, CsTe, Te, Te_2, $ZrTe_2$ or Cs_2TeO_3 according to the oxygen potential [1–3]. Recently, some light water reactor fuels have been irradiated to a burn-up of over 50 GWd/t. This means that fuel loading time is elongated and the oxygen potential of fuel is increased step-by-step with that time. As a result, in such fuel rods, it is expected that a certain amount of tellurium or its compound as gaseous species diffuses from the fuel core to the fuel-cladding gap and subsequently reacts with Zircaloy, which is a kind of so-called 'fuel-cladding chemical interaction (FCCI)'. On the other hand, during a reactor accident, tellurium is possible to be released to the environmental system because of its high volatility [4]. Consequently, it would be harmful to health of lives. Considering the problems described above, reaction of Zircaloy with tellurium can be crucially important for the safety of a nuclear reactor.

Various experiments have been so far made on chemical reactions of tellurium with zirconium and zirconium alloys [5,6]. Dependence of chemical forms of tellurium compounds on temperature and weight ratio of Te to Zircaloy-4 was studied by de Boer and Cordfunke [5]. Pulham et al. reported that corrosion depth of Zircaloy-4 increased with increase of oxygen potential [6]. In those reports, tellurium vapor pressure seems to have been relatively high comparing with the one expected in fuel-cladding gap during the normal operating condition of fuel rods and, while the kinetics of corrosion behavior were not so much discussed in detail.

In this study, corrosion behavior of Zircaloy-4 has been investigated at temperature of −600 °C under the oxygen potential of less than or equal to −430 kJ/mol and the tellurium vapor pressure of 3.1×10^{-4} to 2.8×10^{-3} atm. Oxygen potential was controlled by buffer

* Corresponding author. Tel.: +81-92 642 3779; fax: +81-92 642 3800.

E-mail address: arimatne@mbox.nc.kyushu-u.ac.jp (T. Arima).

PII: S0022-3115(02)00711-0

materials to simulate that of the fuel-cladding gap. Corrosion depth of samples was measured with the scanning-electron microscopy (SEM). And simultaneously, distributions of Zr, O and Te were observed with the energy dispersive X-ray (EDX) examination. In addition, chemical forms of corrosion layers were identified with the X-ray diffractometry (XRD). On the basis of the data obtained in these measurements, reaction of Zircaloy-4 was discussed in terms of oxygen potential, tellurium vapor pressure and corrosion time.

2. Experimental

The specimens of Zircaloy-4 used in this experiment were cut from the α-forged rod, and were prepared into the form of a disk which has the geometry of 5 and 0.5 mm thickness. Their surfaces were polished on abrasive papers and then subsequently finished by alumina buffing.

The corrosion tests were carried out by heating each specimen together with the buffer and tellurium in a silica tube evacuated to $\sim 10^{-3}$ Torr. Fig. 1 shows the schematic diagram of experimental set-up. It should be noted that the temperature of tellurium powders was set to be the lowest in the system in order for its vapor not to condense in the middle way to Zircaloy-4 specimen and the buffer. The Zircaloy-4 specimen and the buffer consisting of an equimolar mixture of a metal with its oxide, such as Cr/Cr_2O_3 ($\Delta\overline{G}_{O_2} = -600$ kJ/mol), NbO_2/Nb_2O_5 (−500 kJ/mol) or Mo/MoO_2 (−430 kJ/mol), were placed at the upper side in the sealed tube and were heated at 600 °C, while crushed tellurium powders were placed at the bottom and were heated in the temperature range of 460–550 °C. The tellurium vapor pressure thus obtained was 3.1×10^{-4}–2.8×10^{-3} atm [7]. The samples were analyzed by SEM + EDX and XRD immediately after the corrosion test was completed.

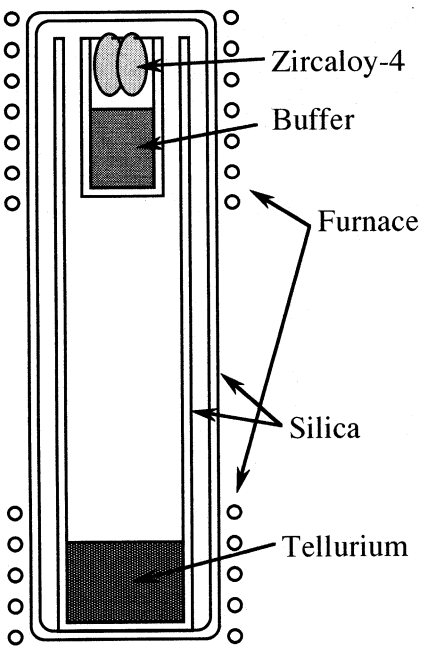

Fig. 1. Schematic diagram of experimental set-up for corrosion tests.

For SEM examinations, the cross-sections of samples embedded in an acrylic resin were observed. The surfaces of the observed sections were mechanically polished as described above, and subsequently were measured the corrosion depth and distribution of elements. For EDX examinations, characteristic X-rays of Zr-Lα, O-Kα and Te-Lα were detected.

In order to investigate the chemical form of corrosion layers, X-ray diffraction measurements were performed. X-ray patterns from corroded samples were acquired using an XD-D1 Shimadzu diffractometer. The diffractometer was used with Cu-Kα radiation at conditions of 40 keV and 30 mA. All X-ray diffraction measurements were performed at room temperature.

3. Results and discussion

Fig. 2 shows the SEM photograph of cross-sectional view of sample corroded under the condition of Cr/Cr_2O_3 buffer with tellurium vapor pressure of 8.9×10^{-4} atm for 24 h as well as results from line analysis by EDX examination. The duplex corrosion layer was formed on the surface of Zircaloy-4 specimen. This is a typical SEM photograph for the sample corroded under the low oxygen potential, i.e. NbO_2/Nb_2O_5, Cr/Cr_2O_3 buffers and no oxygen buffer, with tellurium vapor. By the EDX examination, the inner corrosion layer consisted of Zr and Te, whereas the outer corrosion layer consisted of Zr and O. On the other hand, in case of using Mo/MoO_2 buffer with tellurium vapor pressure of 8.9×10^{-4} atm for 24 h, a single layer was observed by SEM (Fig. 3). EDX examination clarified that this layer consisted of Zr and O, and that Te was not included.

The X-ray diffraction patterns from corrosion layers were taken over the 2θ range of 20–80°. Fig. 4(a) shows the diffraction pattern from the sample corroded under the oxygen potential of −600 kJ/mol and tellurium vapor pressure of 8.9×10^{-4} atm. As shown in this figure, both ZrTe and ZrO_2 peaks were observed. For the sample corroded under the oxygen potential of −430 kJ/mol and tellurium vapor pressure of 8.9×10^{-4} atm, ZrO_2 peaks from the corrosion layer and α-Zr peaks from underlying Zircaloy-4 were observed as shown in Fig. 4(b).

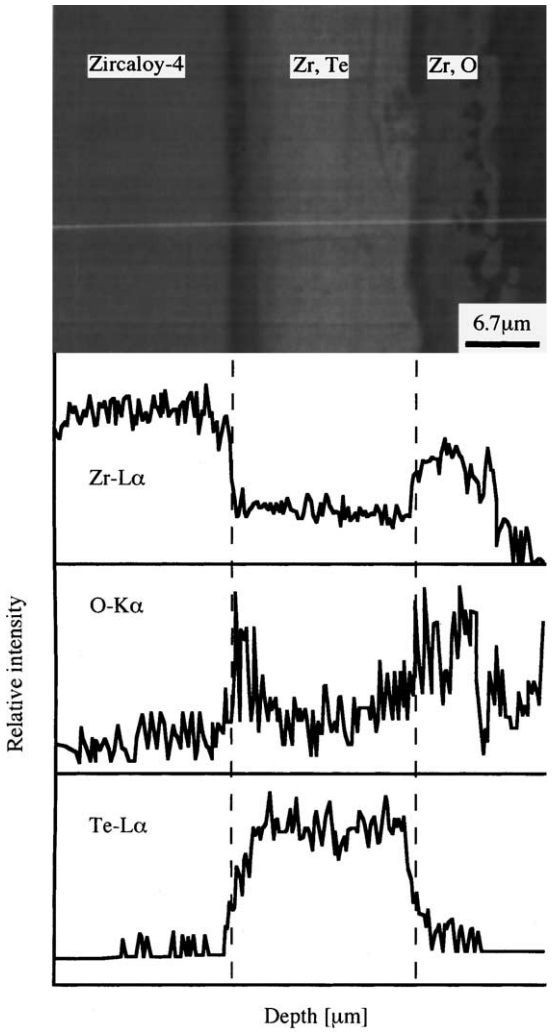

Fig. 2. SEM photograph of cross-sectional view of sample corroded under the oxygen potential of −600 kJ/mol with tellurium vapor pressure of 8.9×10^{-4} atm for 24 h. Results from line analysis of EDX examinations are shown.

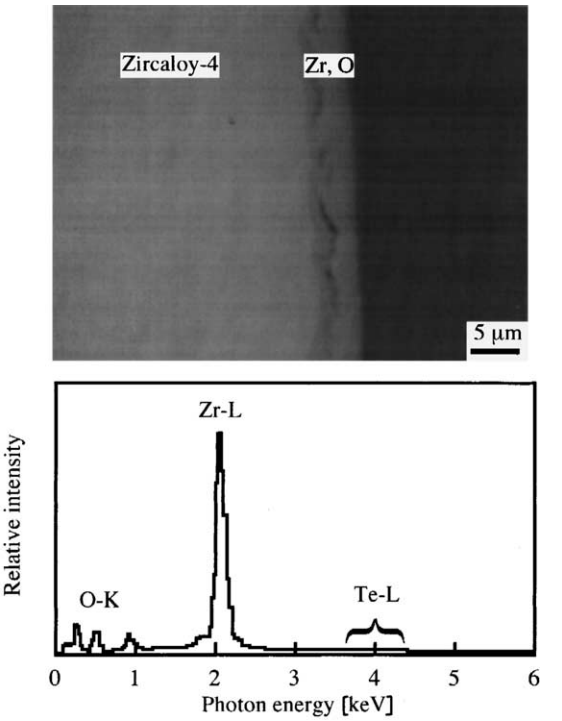

Fig. 3. SEM photograph of cross-sectional view of sample corroded under the oxygen potential of −430 kJ/mol with tellurium vapor pressure of 8.9×10^{-4} atm for 24 h. Corrosion layer was analyzed by EDX examination.

Effect of oxygen potential on growth of corrosion layer was shown in Fig. 5. For corrosion layer which consisted of oxide and telluride, thickness of each layer was plotted as a function of time. These samples were corroded with tellurium vapor pressure of 8.9×10^{-4} atm. Thickness of oxide obtained under NbO_2/Nb_2O_5 buffer was thicker than that under Cr/Cr_2O_3 buffer. On the contrary, thickness of telluride obtained under Cr/Cr_2O_3 buffer was thicker than that under NbO_2/Nb_2O_5 buffer. In addition, we performed the corrosion test without oxygen buffer for 24 h. In this case, of which oxygen potential was extremely low, the duplex layer was also observed to form. Thickness of the oxide was about 3 μm and that of telluride was 30 μm. It was considered that the activity of oxygen increases in the high oxygen potential, while that on the contrary, that of tellurium does in the low oxygen potential.

In order to discuss the process of growth for such duplex layers which was observed under the low oxygen potential, SEM photographs of sample corroded for the short time of 6 h were taken, which are shown in Fig. 6. Fig. 6(a) shows the single layer as well as the duplex layer, which means that formation of duplex layers was not completed. In this figure, the single layer was identified to be composed of zirconium oxide, while the duplex layer consisted of oxide and telluride. On the other hand, Fig. 6(b) shows only the duplex layer. These SEM photographs were taken for the same corroded sample. For the corrosion time of 6 h, difference in the degree of corrosion can be seen in one sample. The growth process of the duplex layer is briefly summarized as follows. In the initial stage of corrosion, the oxide layer covered the specimen. And subsequently, the telluride layer started to grow by the reaction of zirconium in the underlying Zircaloy-4 with tellurium coming through the oxide layer. After that, the telluride layer thickened between underlying Zircaloy-4 and the oxide layer. Only from our experimental results, it cannot be determined whether the telluride formation occurs

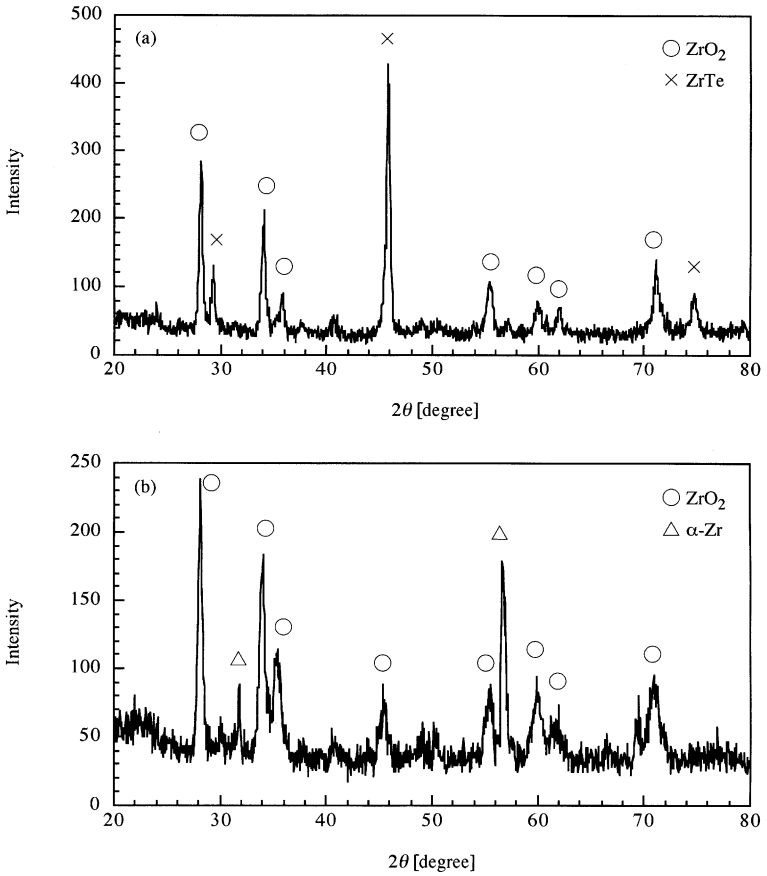

Fig. 4. X-ray diffraction patterns from sample corroded with tellurium vapor pressure of 8.9×10^{-4} atm at the oxygen potential of (a) −600 kJ/mol and (b) −420 kJ/mol.

between underlying Zircaloy-4 and the telluride layer or between the telluride and oxide layers. For the growth of oxide, in addition to the oxide formed at the initial stage of corrosion, telluride seems to be oxidized in the vicinity of the oxide layer formed in the initial stage of corrosion, and consequently oxide is newly grown with time. To verify this model, the pre-oxidized sample was corroded with tellurium under the Cr/Cr_2O_3 buffer. Pre-oxidized sample was prepared by heating at 600 °C for 24 h under the Mo/MoO_2 buffer 'without' tellurium vapor. By this treatment, the oxide layer in about 5 μm thickness covered the specimen. Fig. 7 shows the result from corrosion test of pre-oxidized sample. Pre-oxide, oxide newly grown from telluride and telluride are observed in this figure. The similar triplex corrosion layer is also seen in Fig. 6(b). A series of these corrosion tests indicates not only the growth process of corrosion layer but also that the oxide layer might not be protective in the low oxygen potential against chemical attack by tellurium.

Fig. 8 shows the effect of tellurium vapor pressure on growth of corrosion layer. At the oxygen potential of −600 kJ/mol, thickness for oxide or telluride was increased with tellurium vapor pressure. Comparison of oxide thicknesses observed with or without tellurium vapor is shown in Fig. 9, which elucidates the effect of tellurium vapor on oxidation of Zircaloy-4. Data points plotted in Fig. 9 were obtained from the corrosion tests in tellurium vapor which were carried out with the buffer applied in this study. In addition, weight gain curves for Zircaloy-4 samples oxidized in CO/CO_2 gas mixture, of which oxygen potential was −300 to −10 kJ/mol, are shown in it [8]. As shown in Figs. 8 and 9, tellurium vapor obviously promoted the oxidation of Zircaloy-4. Even if the value of oxygen potential controlled by buffer was the same, the obtained oxide thickness was larger for higher tellurium vapor pressure cases. Accordingly, it can be imagined that zirconium telluride might be easily oxidized in the oxidizing atmosphere.

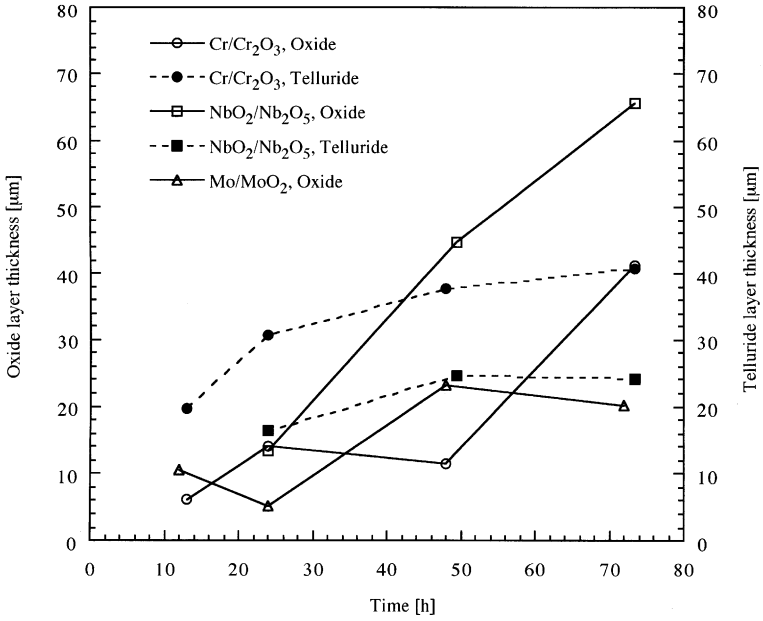

Fig. 5. Effect of oxygen potential on growth of corrosion layer.

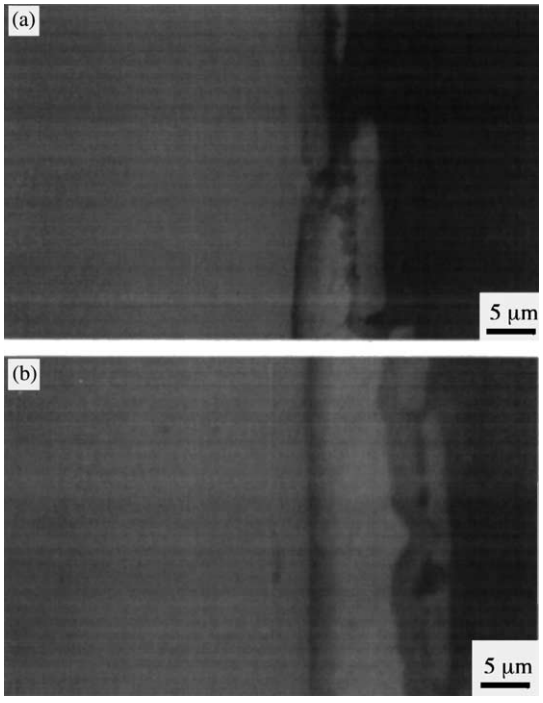

Fig. 6. SEM photograph of cross-sectional view of sample corroded under the oxygen potential of −600 kJ/mol with tellurium vapor pressure of 8.9×10^{-4} atm for 6 h. (a) Single and duplex corroded layers and (b) duplex (or triplex?) layer.

Here, formation of corrosion layer was considered from the point of view of chemical-equilibrium theory.

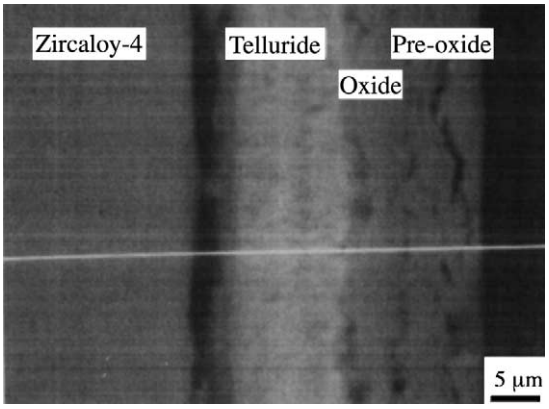

Fig. 7. SEM photographs of cross-sectional view of pre-oxidized sample corroded under the oxygen potential of −600 kJ/mol with tellurium vapor pressure of 8.9×10^{-4} atm for 24 h. Before corrosion test with Te, the sample was oxidized under the oxygen potential of −430 kJ/mol for 24 h.

For this purpose, a stability diagram for Zr–Te–O system is available [9–11]. Fig. 10 shows the stability diagram at the temperature of 600 °C under low oxygen partial pressures. In order to draw this figure, equations listed in Table 1 had to be solved. For instance, to draw the boundary line between two solid phases, $ZrTe_3$ and ZrO_2, reaction of no. 5 must be solved as a function of oxygen partial pressure and tellurium vapor pressure. As can be seen in this diagram, even under the lowest oxygen potential, Cr/Cr_2O_3 buffer, telluride cannot be

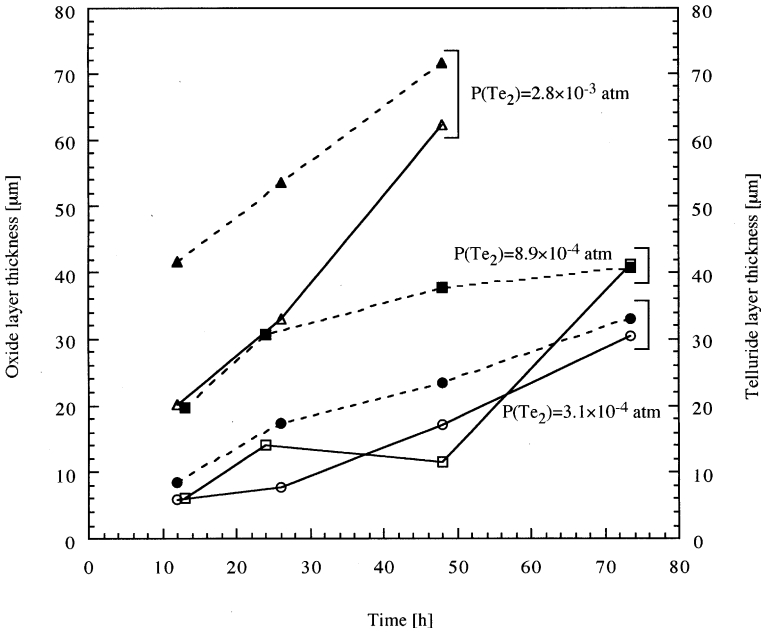

Fig. 8. Effect of tellurium vapor pressure on growth of corrosion layer. Open and solid symbols stand for oxide and telluride, respectively.

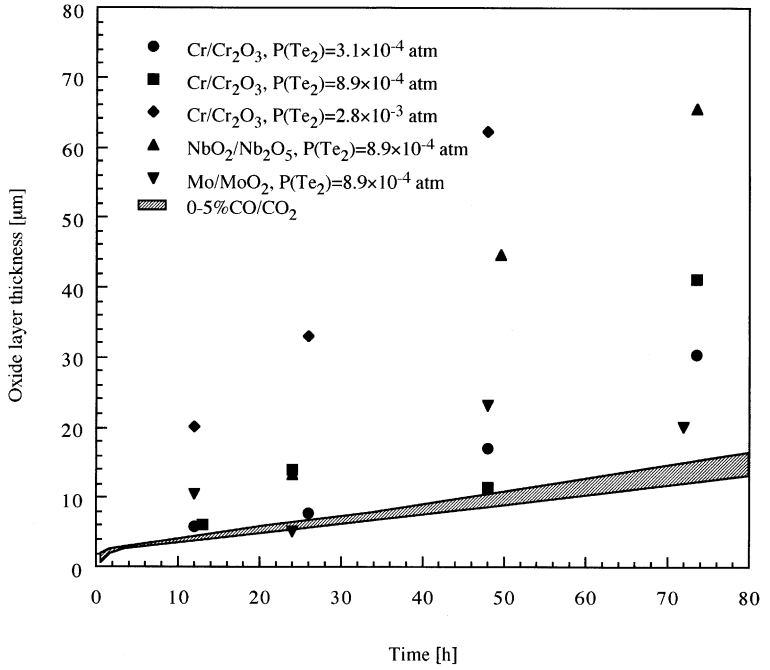

Fig. 9. Effect of tellurium vapor on oxidation of Zircaloy-4.

formed. A further lower oxygen potential is considered to be needed to form zirconium telluride. However, in this study, telluride layers were observed to form under the condition of using Cr/Cr_2O_3 or NbO_2/Nb_2O_5 buffers, not to mention the condition without using oxygen buffer. It is naturally interpreted that, when telluride

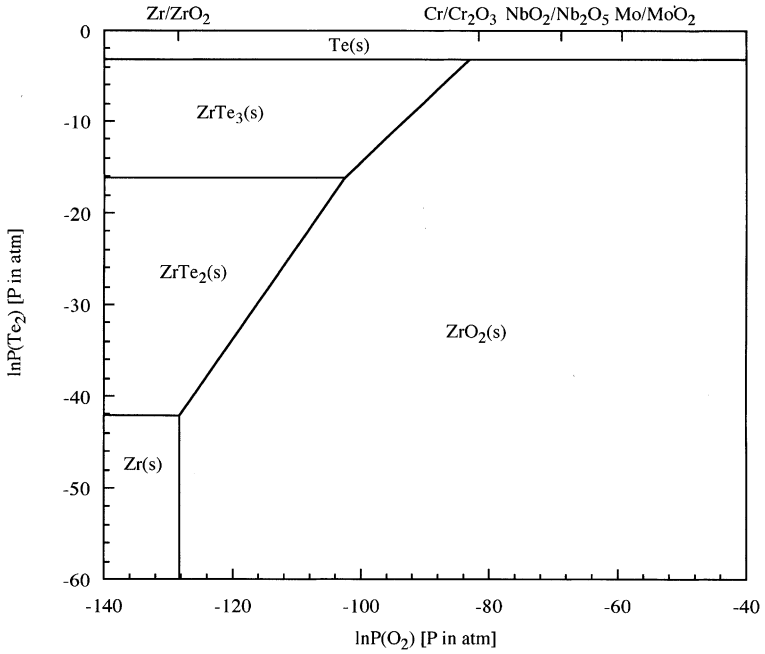

Fig. 10. Stability diagram for Zr–Te–O system at 600 °C.

Table 1
Chemical reactions in Zr–Te–O system

No.	Reaction
1	$Zr(s) + O_2 = ZrO_2(s)$
2	$ZrTe_2(s) + O_2 = Te_2(g) + ZrO_2(s)$
3	$Zr(s) + Te_2(g) = ZrTe_2(s)$
4	$ZrTe_2(s) + 1/2\ Te_2(g) = ZrTe_3(s)$
5	$ZrTe_3(s) + O_2 = 3/2\ Te_2(g) + ZrO_2(s)$
6	$1/2\ Te_2(g) = Te(s)$
7	$ZrO_2(s) + 3/2\ Te_2(g) + 3O_2 = ZrTe_3O_8(s)$
8	$1/2\ Te_2(g) + O_2 = TeO_2(s)$
9	$Te(s) + O_2 = TeO_2(s)$

layer is formed, the oxygen potential to be established by underlying Zircaloy-4 and the outer oxide should be as low as that of Zr/ZrO_2, i.e. ~ -930 kJ/mol. Concerning the composition of zirconium telluride, the ratio of Te to Zr was approximately 1:1 for the telluride layer by EDX. In addition, as shown in Fig. 4(a), telluride formed in this study was seemed to be ZrTe under the oxygen potential of -600 kJ/mol. According to the stability diagram for Zr–Te–O system (Fig. 10), our experimental condition would not allow ZrTe to form but $ZrTe_3$. Chemical form of telluride on corroded Zircaloy-4 is also discussed in Refs. [5,6]. Those reports show the tendency that, when temperature is high or tellurium vapor pressure is low, zirconium-rich tellurium compound, e.g. Zr_5Te_4, can be formed [5]. From the aspect of oxygen partial pressure, ZrTe can be observed under the low oxygen partial pressure, while ZrO_2 or $ZrO_2 + ZrTe$ can be done under the high oxygen partial pressures [6]. In our experiments, the oxygen potential was controlled by the buffer, and the reaction temperature is relatively high. Furthermore, the chemical form of tellurium concerned with corrosion is vapor. Therefore, ZrTe was observed in our experiment because of high temperature of reaction and low vapor pressure of tellurium. In addition, kinetic factors, such as diffusion of tellurium through ZrO_2 layer, may have effect on the formation of telluride. As a result, a plenty amount of tellurium might not be supplied to form the compound of $ZrTe_3$.

4. Conclusion

In this study, reaction of Zircaloy-4 with tellurium vapor has been studied at 600 °C under different oxygen potentials as controlled by the buffer such as Cr/Cr_2O_3, NbO_2/Nb_2O_5 or Mo/MoO_2. Under the low oxygen potential less than -500 kJ/mol, duplex corrosion layers were observed to form, which consisted of zirconium telluride and zirconium oxide. About growth of corrosion layer, its thickness was increased with time and tellurium vapor pressure. An attempt to explain the formation of such duplex corrosion layers was made from the point of view of both chemical-equilibrium and kinetic models. On the other hand, under a high oxygen potential of -430 kJ/mol, only zirconium oxide was formed on the surface of Zircaloy-4 specimen.

Acknowledgements

The authors gratefully acknowledge the continuous support by the technical staff, M. Momoda and M. Kutsuwada. We also wish to thank M. Watanabe of the Center of Advanced Instrumental Analysis, Kyushu University, for her help with the X-ray diffraction measurements.

References

[1] E.H.P. Cordfunke, R.J.M. Konings, J. Nucl. Mater. 152 (1988) 301.
[2] R.G.J. Ball, W.G. Burns, J. Henshaw, M.A. Mignanelli, P.E. Potter, J. Nucl. Mater. 167 (1989) 191.
[3] E.H.P. Cordfunke, R.J.M. Konings, J. Nucl. Mater. 201 (1993) 57.
[4] O. Götzmann, J. Nucl. Mater. 201 (1993) 267.
[5] R. de Boer, E.H.P. Cordfunke, J. Nucl. Mater. 223 (1995) 103.
[6] R.J. Pulham, M.W. Richards, D.R. Kennard, J. Nucl. Mater. 223 (1995) 277.
[7] O. Kubaschewski, C.B. Alcock, Metallurgical Thermochemistry, 5th Ed., Pergamon, New York, 1979.
[8] T. Arima, T. Masuzumi, H. Furuya, K. Idemitsu, Y. Inagaki, J. Nucl. Mater. 294 (2001) 148.
[9] S. Yamanaka, N. Takatsuka, M. Katsura, M. Miyake, J. Nucl. Mater. 161 (1989) 210.
[10] S. Yamanaka, M. Katsura, M. Miyake, Technol. Rep., Osaka University, vol. 38, 1988, p. 59.
[11] K.C. Mills, Thermodynamic Data for Inorganic Sulphides, Selenides, and Tellurides, Butterworths, London, 1974.